3468

名古屋大学図書
洋 1026252

Space-Charge Layer Width and Junction Capacitance of a Hyper-Abrupt p-n Junction

By Hideo NUKUSHINA

Japan Radio Company, Ltd., 5th Mori-Building, 25, Shiba-Nishikubo-Sakuragawa-cho, Minato-ku, Tokyo

The space-charge layer width and the junction capacitance of a hyper-abrupt p-n junction were studied, especially on the characteristics of temperature-dependence. The solution of Shockley's equation in space-charge case gives a fairly good approximation of the characteristics of such a junction. The temperature dependence of the space-charge layer width can be explained mainly by the change in the built-in barrier voltage. However, there still remains a tendency that, at higher temperature, the space-charge layer width is lower than that of the expected magnitude.

§ 1. Introduction

The recent development on fabricating semiconductor junction diodes and transistors makes it possible to form a various kinds of $p-n$ or $n-p$ junctions, by means of combined alloy-diffusion process or vapor-growth technique. The "hyper-abrupt" junction, the name of which was given by McMahon and Straube [1], is one of these products, and is essentially an abrupt junction but, different from the ordinary abrupt junction, the impurity concentration on one side of the junction is inversely graded. The emitter junction of the alloy-diffusion transistor conforms to the shape of this junction, and as Frazier [2] proposed, this junction can be used as a voltage-controlled capacitance diode of an improved sensitivity.

In this paper, we describe results of the study of the characteristics of this junction biased to reversed polarity, especially on the space-charge layer width and the junction capacitance. The distinguishing nature of the hyper-abrupt junction is the sharp dependence of space-charge layer width on the applied voltage. We start from the assumption that the distribution of the impurity concentration on the n-type side is exponential, and obtain the relation between the space-charge layer width and the voltage across the junction in a general form by solving space-charge equation. Then experimentally obtained characteristics of temperature-dependence are shown and the characteristics are analysed and explained by the temperature-dependence of the built-in barrier voltage. Finally, the disagreement between the theoretical study and the experimental results will be discussed in qualitative arguments.

§ 2. Space-Charge Layer Width and Junction Capacitance.

In a hyper-abrupt $p-n$ junction, which we are concerned with, the conductivity type varies abruptly from a heavily doped p to a moderately doped n and then sharply decreases to a less conductive n-type. In analysing the potential distribution and the junction capacitance of such a junction, we assume that the acceptor concentration on the p-type side is much greater than the donor concentration at any point on the n-type side, thus all of the space-charge region will essentially be on the n-type side. We further assume that the distribution of the donor concentration on the n-type side is exponential. The donor distribution may then be given by

$$N(x) = N_0 e^{-\alpha x} + N_1 \qquad (2.1)$$

in which N_0 is the donor concentration just adjacent to the abrupt junction, N_1 is that at the region extremely far from the junction, and x is the distance from the abrupt junction toward into the n-type side.

To obtain the potential function $\psi(x)$, and hence the effective space-charge layer width, in a thermal equilibrium or a pseudo-equilibrium condition, we have to solve Shockley's equation which is of the form [3]

$$\frac{d^2u}{dx^2} = \frac{1}{K}[\sinh u - \rho(x)] \qquad (2.2)$$

Although it has been proved that an unique solution exisits for this equation for any realizable distribution of the impurity concentration, it is

generally impossible to obtain the solution of this non-linear equation by an analytical method. Accordingly, as in the usual approximate method for obtaining the solution of the junction equation, we assume here, as shown in Fig. 2.1, that the transition region of the junction can be divided into three regions in such a way that the region of fixed space-charges without mobil carriers, extending from $x = 0$ to $x = x_1$, is bounded by semi-infinite neutral zones. We should note here, however, that there is no justification for such a configuration of charge distribution being permissible, and actually, the true neutral condition will be established only at a great distance from the abrupt junction while the space-charge condition will be valid only at a region extremely close to the junction. The accuracy of the approximation should therefore be checked later.

Now, according to the approximations described above, the potential function should satisfy Poisson's equation of the form,

$$\frac{d^2\psi}{dx^2} = -K(e^{-\alpha x} + \delta) \qquad (2.3)$$

where,

$$K = \frac{qN_0}{\varepsilon} \quad , \qquad \delta = \frac{N_1}{N_0} \qquad (2.4)$$

in which q is the electronic charge and ε the dielectric constant of the base semi-conductor. We note here that, in the above equations and throughout this paper hereafter, we adopt the rationalized M.K.S. unit system.

The boundary conditions for Eq. (2.3) are

$$\text{at } x=0: \quad \frac{d\psi}{dx} = \text{finite}, \quad \psi = 0 \tag{2.5}$$

$$\text{at } x=x_1: \quad \frac{d\psi}{dx} = 0, \quad \psi = V_a + V_i \tag{2.6}$$

where V_a is the magnitude of the reverse voltage across the junction and V_i is the built-in potential difference. V_i is considered to be the difference between the potentials in the neutral sides at $x=0$ and $x=x_1$, respectively. Thus, V_i is expressed, with a fairly good approximation, as

$$V_i = \frac{kT}{q} \ln\left[\frac{N_p N_o}{n_i^2}\left(e^{-\alpha x} + \delta\right)\right] \tag{2.7}$$

when the donors and acceptors are completely ionized.

Eq. (2.3) with the boundary conditions (2.5) and (2.6) can be easily integrated:

$$\frac{d\psi}{dx} = K\left[\frac{1}{\alpha}\left(e^{-\alpha x} - e^{-\alpha x}\right) - \delta(x - x_1)\right] \tag{2.8}$$

$$\psi = K\left[\frac{1}{\alpha^2}\left(1 - e^{-\alpha x}\right) - \frac{x}{\alpha}e^{-\alpha x} - \frac{\delta}{2}x^2 - \delta x x_1\right] \tag{2.9}$$

$$V_a + V_i = K\left[\frac{1}{\alpha^2}\left(1 - e^{-\alpha x_1}\right) - \frac{x_1}{\alpha}e^{-\alpha x_1} + \frac{\delta}{2}x_1^2\right] \tag{2.10}$$

or rearranging Eq. (2.10),

$$V_a + V_i = \frac{K}{\alpha^2}\left[1 - e^{-\alpha x_1}(1 + \alpha x_1) + \frac{\delta}{2}(\alpha x_1)^2\right] \tag{2.11}$$

Inserting (2.7) into the left-hand side of Eq. (2.11), we have

$$V_a + V_{i0} + \frac{kT}{q} \ln (e^{-\alpha x_1} + \delta) = \frac{K}{\alpha^2} [1 - e^{-\alpha x_1}(1 + \alpha x_1) + \frac{\delta}{2}(\alpha x_1)^2] \quad (2.12)$$

where

$$V_{i0} = \frac{kT}{q} \ln \frac{N_p N_0}{n_i^2} \quad (2.13)$$

Because Eq. (2.11) or (2.12), which shows the relation between the space-charge layer width and the junction voltage, is of a transcendental form, it is difficult to write down the space-charge layer width as an explicit function of the voltage across the junction. Accordingly, before computing numerically, we will investigate some qualitative characteristics of this junction by considering extreme cases.

First, we assume that $\delta = 0$, i.e., the base semiconductor is intrinsic, then Eq. (2.11) becomes

$$V_a + V_i = \frac{K}{\alpha^2} [1 - e^{-\alpha x_1}(1 + \alpha x_1)] \quad (2.14)$$

When αx_1 is small compared to unity, i.e., the voltage across the junction is very small, Eq. (2.14) can be written as

$$V_a + V_i = \frac{K}{2} x_1^2 \quad (2.15)$$

In deriving Eq. (2.15), we use the Tayler expansion of an exponential function:

$$e^{-\alpha x} = 1 - \alpha x + \frac{(\alpha x)^2}{2!} - \frac{(\alpha x)^3}{3!} - \cdots\cdots$$

and neglect the terms higher than $(\alpha x)^3$. Eq. (2.15) shows that, when x_1 is small the relation between the space-charge layer width and the voltage across the junction follows the square law which holds for a simple abrupt junction.

On the contrary, when αx_1 is large compared to unity, i.e., the voltage across the junction is large, Eq. (2.11) can be written

$$V_a + V_i = \frac{K}{\alpha^2}(1 - \alpha x_1 e^{-\alpha x_1}) \qquad (2.16)$$

Now, the quantity $1/\alpha$ is the distance in which the impurity concentration falls to $1/e$ of its original value. On the other hand, the space-charge layer width of a simple abrupt junction with the donor concentration of is equal to $\sqrt{2V_{i0}/K}$ when no external voltage is applied. We introduce here a parameter ξ which is the ratio of $1/\alpha$ to $\sqrt{2V_{i0}/K}$. In other words, the effective thickness of the heavy doped region in the hyper-abrupt junction is ξ times the width of the natural space-charge layer of a simple abrupt junction with the same value of K. Thus

$$\frac{1}{\alpha} = \xi \left(\frac{2V_{i0}}{K}\right)^{\frac{1}{2}} = \xi d_0 \qquad (2.17)$$

Substituting this relation into (2.16) leads to

$$\frac{V_a + V_i}{V_i} = 2\xi^2 \left[1 - \frac{x_1}{\xi d_0} \exp\left(-\frac{x_1}{\xi d_0}\right)\right] \qquad (2.18)$$

Since $\lim_{z\to\infty} z e^{-z} = 0$, the right-hand side of Eq. (2.18) approaches to $2\xi^2$ when αx_1 increases to infinity. In other words, at the external applied voltage of

$$V_a = V_i(2\xi^2 - 1) \tag{2.19}$$

the space-charge layer width, x_1, becomes infinite.

Finally, we consider the case when $\delta \neq 0$. If δ is small, the third term in the right-hand side of Eq. (2.11) or of its transformed form,

$$\frac{V_a + V_i}{V_i} = 2\xi^2\left[1 - \exp\left(-\frac{x_1}{\xi d_0}\right)\left(1 + \frac{x_1}{\xi d_0}\right) + \frac{\delta}{2}\left(\frac{x_1}{\xi d_0}\right)^2\right] \tag{2.20}$$

does not contribute when x_1 is small. At a considerablly large magnitude of x_1, Eq. (2.20) can be written as

$$\frac{V_a + V_i}{V_i} = 2\xi^2 + \delta\left(\frac{x_1}{d_0}\right)^2 \tag{2.21}$$

This equation shows that, for large value of the junction voltage, the relation between the junction voltage and the space-charge layer width again follows the square law.

The qualitative analysis discussed thus far is illustrated in Fig.2.2. As is shown in the figure, the curve which shows the relation between the space-charge layer width and the junction voltage of a hyper-abrupt junction consists of three parts: square law at a smaller junction voltage, sharper variation at a moderate voltage range and again square law relation in a larger junction voltages.

The capacitance across the space-charge layer is equivalent to that of a parallel-plate condenser of spacing x_1, thus we have

$$C = \frac{\varepsilon A}{x_1}$$

where A is the junction area. Therefore, the variable capacitance characteristics is quite similar to the voltage-dependence of the space-charge layer width discussed above. In Fig. 2.3, the junction capacitance is calculated and plotted for various values of ξ and δ. We note that, in calculating curves in Fig. 2.3, the dependence of the internal barrier voltage to the space-charge layer width as equated in Eq. (2.7) is not taken into account but the barrier voltage is assumed to be constant.

An experimental hyper-abrupt junction diode was fabricated by means of the alloy-diffusion technique. n-type germanium with the specific resistivity of approximately 20 ohm-centimeters (at room temperature) is used as the base material on which Pb containing small amount of Ga and Sb is alloyed to form the junction. An appropriate heat treatment makes antimony atoms to diffuse into the inner side of germanium base, resulting a similar distribution of donors previously discussed, while the gallium atoms remain in the Pb-Ga alloy, forming the heavily doped p-region. From the atomic percentage of Ga in Pb, the acceptor concentration in the p-region is estimated to be the order of $10^{25}/\text{meter}^3$.

The variable capacitance characteristics of this diode at room temperature is shown in Fig. 2.4. Using the actual value of the junction area of this diode, 7.1×10^{-4} cm^2, the effective space-charge layer width as a function of the applied voltage is obtained and plotted in Fig. 2.5.

In the figure, the dotted line is the experimental curve on which measured points are plotted, while the solid line shows the theoretical curve given by Eq. (2.12) with $\alpha^{-1} = 0.12 \times 10^{-6}$ meters, $K = 1.8 \times 10^{14}$ coulomb per farad.meter, and $\delta = 3.5 \times 10^{-3}$, respectively. The agreement between the experimental values and the theoretical curve is fairly good. For the magnitude of V_i used in the computation, it will be described in details in the next section.

The temperature and the period of heat treatment for the donors to diffuse into the base germanium was chosen to be $T = 700^{\circ}C$ and $\tau = 8$ minutes, respectively. Assuming that the diffusion constant of antimony in germanium is 1.0×10^{-12} cm^2/sec., the gradient of the donor distribution may be estimated as $\alpha^{-1} = 0.11 \times 10^{-6}$ meters. The agreement between this value of α^{-1} and that used in the analysis of the actual relation of the space-charge layer width vs junction voltage shown in Fig. 2.5 may be considered to be good. On the other hand, from the atomic percentage of Sb in Pb, the concentration of donors at the alloy-front, i.e., $x = 0$, is estimated to be approximately 3×10^{24}/meter^3 if an ideal alloy-diffusion process is achieved, while $K = 1.8 \times 10^{14}$ coulomb/farad.meter^2 which is adopted to the theoretical curve in Fig. 2.5 corresponds to $N_o = 1.58 \times 10^{23}$/meter^3. However, a considerable reduction in the concentration of donors at the alloy-front can be expected because of the cancellation of donors by diffused Ga atoms or the advancement of alloy region into n-side during the period of heat treatment for diffusion at lower temperature. Accordingly, as the donor concentration at the alloy-front, 1.58×10^{23}/meter^3 may be believed to be a more reasonable value than 3×10^{24}/meter^3 which is estimated for the ideal alloy-diffusion process.

If we approve of the donor concentration at the alloy-front being $1.58 \times 10^{23}/\text{meter}^3$, $\delta = 3.5 \times 10^{-3}$ leads to $N_1 = 5.53 \times 10^{20}/\text{meter}^3$. (as previously stated, N_1 is the donor concentration at a distance extremely far from the junction). The specific resistivity of 20 ohm.centimeters at room temperature corresponds to the donor concentration of $6 \times 10^{19}/\text{meter}^3$. However, the magnitude of this specific resistivity is that measured before treatment. We may expect some change in resistivity or donor concentration through a various process of heat treatment. Moreover, as it will be discussed in the next section, there is a tendency that the apparent magnitude of δ becomes larger than the actual ratio of minimum to maximum concentration of impurities in the n_1-type region.

§ 3. Temperature-Dependence of the Space-Charge Layer Width

As well as the characteristics of the hyper-abrupt junction diode at the room temperature (300° K), those at temperatures of 70° K, 200° K and 350° K, respectively, were also investigated. The junction capacitance and the space-charge layer width at these temperatures are shown in Fig. 3.1 and Fig. 3.2, respectively, for the same diode as illustrated in the previous section.

To analyze the temperature-dependence of the space-charge layer width, we have to consider factors which depend on temperature. As the primary consideration, dependence of the barrier voltage, V_i , on temperature would be the most effective factor to the variation of the space-charge layer width.

In the previous section we gave the barrier voltage, V_i , in the form

$$V_i = \frac{kT}{q} \ell_n \frac{N_p N_o (e^{-\alpha x} + \delta)}{n_i^2}$$

In giving this equation, we assumed that all the acceptors and donors are completely ionized. In this section, we give up this assumption and start from the original situation to derive the barrier voltage of a $p-n$ junction. ~~As is shown in Fig. 3.3~~, The barrier voltage in the equibrium condition is given by

$$V_{io} = E_g - (E_p^* + E_n^*) \qquad (3.1)$$

in which

$$E_p^* = \frac{1}{2}\left(E_A - \frac{kT}{q}\ln\frac{N_A^*}{p^*}\right) \tag{3.2}$$

$$E_n^* = \frac{1}{2}\left(E_D - \frac{kT}{q}\ln\frac{N_D^*}{n^*}\right) \tag{3.3}$$

$$n^* = 2\left[\frac{2\pi m^* kT}{h^2}\right]^{\frac{3}{2}} = 4.82\times10^{15}T^{\frac{3}{2}}/cm^3 \tag{3.4}$$

$$p^* = 2\left[\frac{2\pi m^* b\, kT}{h^2}\right]^{\frac{3}{2}} \tag{3.5}$$

where,

E_g = energy gap (width of the forbidden band)

E_p^* = difference between the Fermi level and the top of the valence-bond band

E_n^* = difference between the Fermi level and the bottom of the conduction band

E_A = difference between the acceptor level and the top of the valence-bond band

E_D = difference between the donor level and the bottom of the conduction band

N_A^* = density of the ionized acceptor

N_D^* = density of the ionized donor

p^* = effective density of states of holes in the valence-bond band

n^* = effective density of states of electrons in the conduction band

m^* = effective mass of electron

b = effective hole-electron mass ratio $\doteqdot 2$

Among these quantities, N_A^* and N_D^* are determined by the following two equations, respectively,

$$\frac{N_A^*}{N_A - N_A^*} = p^* \exp\left[-\frac{E_A}{kT}\right] \qquad (3.6)$$

$$\frac{N_D^*}{N_D - N_D^*} = n^* \exp\left[-\frac{E_D}{kT}\right] \qquad (3.7)$$

When we assume both E_A and E_D are 0.01 volts and apply Eqs. (3.6) and (3.7) with Eqs. (3.4) and (3.5) to our experimental diode in which $N_A = 10^{25}/\text{meter}^3$ and $N_D = 1.58 \times 10^{23}/\text{meter}^3$, we find that, at 70° K, acceptor atoms are not fully ionized but about 70% of them are ionized or 30% of them are still reserved and, at the alloy-front, 20% of the donor atoms are still reserved, however, in the n-type region where the donor concentration is less than $10^{22}/\text{meter}^3$, donor atoms are almost fully ionized or exausted. On the other hand, at the temperature of 200° K or higher, both acceptor atoms and donor atoms are fully ionized or exausted.

Taking these situations into consideration, successive computations of Eqs. (3.4), (3.5), (3.6), (3.7), then (3.2), (3.3) and finally (3.1) result in Fig. 3.3 which shows the relation between the effective barrier voltage and the space-charge layer width given by

$$V_i = V_{i0} + \frac{kT}{q_D} \ln\left(e^{-\alpha x} + \delta\right)$$

at various temperatures. For the temperature dependence of E_g, we derive the following relation from the experimental data of Conwell[4],

$$E_g = 0.75 - 2.7 \times 10^{-4}\, T(^\circ K) \quad \text{volts} \qquad (3.8)$$

From the dependence of the barrier voltage on temperature as described above, we can see how the characteristics of the space-charge layer width

does depend on temperature. The results are shown in Figs. 3.4, 3.5 and 3.6. The characteristics at 300° K has already shown in Fig. 2.5. In these figures, as similar to Fig. 2.5, dotted lines are experimentally obtained curves on which measured points are plotted, while solid lines are theoretical curves given by Eq. (2.12) with the same values of parameters, α, κ and δ, but V_i of which the effect of temperature variation is taken account.

Through the results shown in Fig. 2.5, Fig. 3.4, Fig. 3.5 to Fig. 3.6, we see that the theoretical curve with the parameter deduced from the data at 300° K gives a good agreement with the experimentally obtained characteristics at 200° K, but at either 70° K or 350° K, there is a considerable disagreement between the two. A further consideration seems to be necessary.

At 70° K, as mentioned previously, the donor atoms on the n-type side are not fully ionized. Donors in the region close to the junction is in a reserved condition, while those in the region far from the junction is in an exausted condition. This leads to the fact that the effective space-charge density at smaller x is decreased, while that at larger x is maintained as it is at higher temperature. Therefore, the gradient of the distribution of donors is effectively reduced. In Fig. 3.4, the dot-dashed line shows the curve given by Eq. (2.12) with $\alpha^{-1} = 0.13 \times 10^{-6}$ meters instead of 0.12×10^{-6} meters. We see clearly a better agreement with the curve given by the reduced gradient of the distribution of donors.

Although a considerable improvement in the analysis of the characteristics of the space-charge layer width at 70° K by the modification in α, there still remains disagreement between the curve obtained from the formula

and the experimental data not only at 300° K but also at 70° K. From Fig. 3.4 and Fig. 3.6, we see evidently that, in the space-charge layer width vs voltage relations, the theoretical curve exceeds over the experimental curve at 350° K while the former is below the latter at 70° K.

The author wishes to explain this tendency as due to the approximate method in solving the junction equation. As it has already been pointed out at the beginning of Section 2, the true solution for the space-charge layer width can only be obtained by solving Schockley's equation of the form of Eq. (2.2), but unfortunately there is no method to solve it analytically in our case. Qualitatively speaking, the space-charge distribution in the true solution will not have a sharp boundary as is assumed in the approximate method of solving the junction equation. Therefore, the space-charge layer width is not a difinite quantity but should rather be counter-measured from the junction capacitance. An attempt of obtaining the true solution of the junction equation by means of a digital computor has been tried by Morgan and Smith [5] for a linearly graded junction, but their result is not applicable to our problem because of the different distribution of impurities. However, we note that the inhomogeneous distribution of ionized donors will produce a drifting field for electrons. In the hyper-abrupt junction, this field will effect on electrons in such a direction as to pull them toward the junction and this force will be much effective at higher temperature because of the easy movement of electrons, and by the presence of such an effect, the effective space-charge layer width will be decreased to a lower magnitude than in the case of the approximate space-charge case. Experimentaly, we can obtain a better agreement between these two by choosing different magnitude of δ for different temperature. Instead of $\delta = 3.5 \times 10^{-3}$, 3.2×10^{-3} for 70°K

and 4.5×10^{-3} for 350° K give almost complete agreements in both cases.

Even in the conventional approximate method of solving the space-charge equation which we accepted hitherto, we overlook the discontinuity of boundary conditions giving the space-charge layer width. The conventional space-charge solution requires to have zero slope at $x = x_1$. Since the neutral solution has a finite slope at $x = x_1$, there arises a discontinuity in $d\psi/dx$ at $x = x_1$. Accordingly, we require an improved method that both the solution and its first derivative are continuous, although a significant improvement in the accuracy of approximation will not be expected by such a method. To obtain such a solution, as well as the Poisson's equation

$$\frac{d^2\psi}{dx^2} = -K(e^{-\alpha x} + \delta) \tag{2.2}$$

we should have another equation for the neutral case

$$n_i \sinh\left[\frac{q\psi}{kT}\right] = K(e^{-\alpha x} + \delta) \tag{3.9}$$

If we neglect the contribution of holes in the neutral region, we have, instead of Eq. (3.9),

$$\psi = \frac{kT}{q} \ln \frac{K}{n_i}(e^{-\alpha x} + \delta) \tag{3.10}$$

and its first derivative

$$\frac{d\psi}{dx} = -\frac{kT}{q} \frac{\alpha e^{-\alpha x}}{e^{-\alpha x} + \delta} \tag{3.11}$$

Now, in solving Poisson's equation, the boundary condition (2.6) has to be

replaced with

$$\text{at } x \; x_1 : \quad \frac{d\psi}{dx} = -\frac{kT}{q}\frac{\alpha e^{-\alpha x_1}}{e^{-\alpha x_1}+\delta} , \quad \psi = V_a + V_i \qquad (3.12)$$

Direct integration of the original equation leads to

$$V_a + V_i = \frac{K}{\alpha^2}\left[1 - e^{-\alpha x_1}(1+\alpha x_1) + \frac{\delta}{2}(\alpha x_1)^2\right] + \frac{kT}{q}\frac{\alpha x_1 e^{-\alpha x_1}}{e^{-\alpha x_1}+\delta} \qquad (3.13)$$

which gives the relation between the space-charge layer width and the junction voltage in a improved approximation. The solution given by Eq. (3.13) has an additive term of the form

$$\frac{kT}{q}\frac{\alpha x_1 e^{-\alpha x_1}}{e^{-\alpha x_1}+\delta}$$

to the first approximate solution given by Eq. (2.12). Although this improved approximate solution does not fix the problem, we can note that the additive term produces an effect to increase the junction voltage to maintain a given space-charge layer width and its effect is directly proportional to temperature. This effect agrees with the experimental fact that the relative decrease of the space-charge layer width from the expected curve is larger at higher temperature.

Acknowledgements

The author wishes to thank Dr. S. Nakajima, Dr. S. Fukagawa, Mr. S. Takahashi for their continuous encouragements throughout this work. He also wishes to express his sincere thanks to Mr. S. Yamashita and Mr. H. Hoshino for active cooperations and helpful discussions and to Mr. H. Hosaka for preparing fabrications and measurements.

References

1) M. E. McMahon and G. F. Straube: I. R. E. Wescon, Part 3, 72, (1958)

2) H. D. Frazier: Semiconductor Products, March 1960, p. 56.

3) W. Shockley: Bell Syst. Tech. Jour., 28, 435, (1949)

4) E. M. Conwell: Proc. I. R. E., 46, 1281, (1958)

5) S. P. Morgan and F. M. Smits: Bell Syst. Tech. Jour., 39, 1573, (1960)

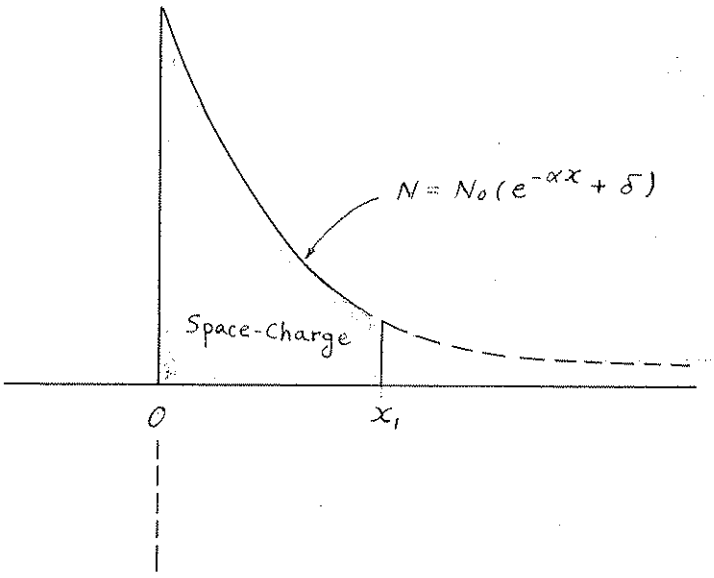

Fig. 2.2 Impurity distribution in the hyper-abrupt p-n junction.

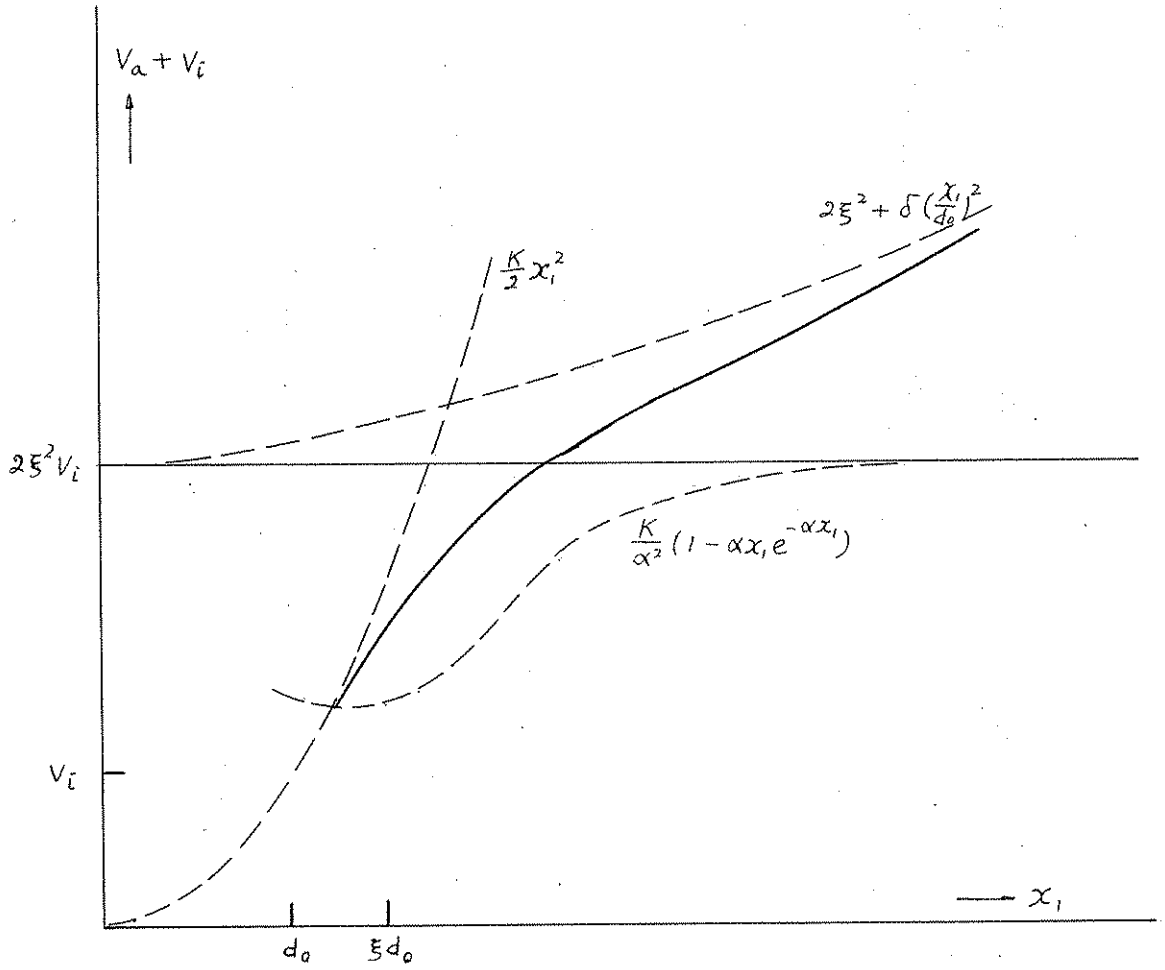

Fig. 2.2 Qualitative analysis of the variation of the space-charge layer width against voltage applied across the junction.

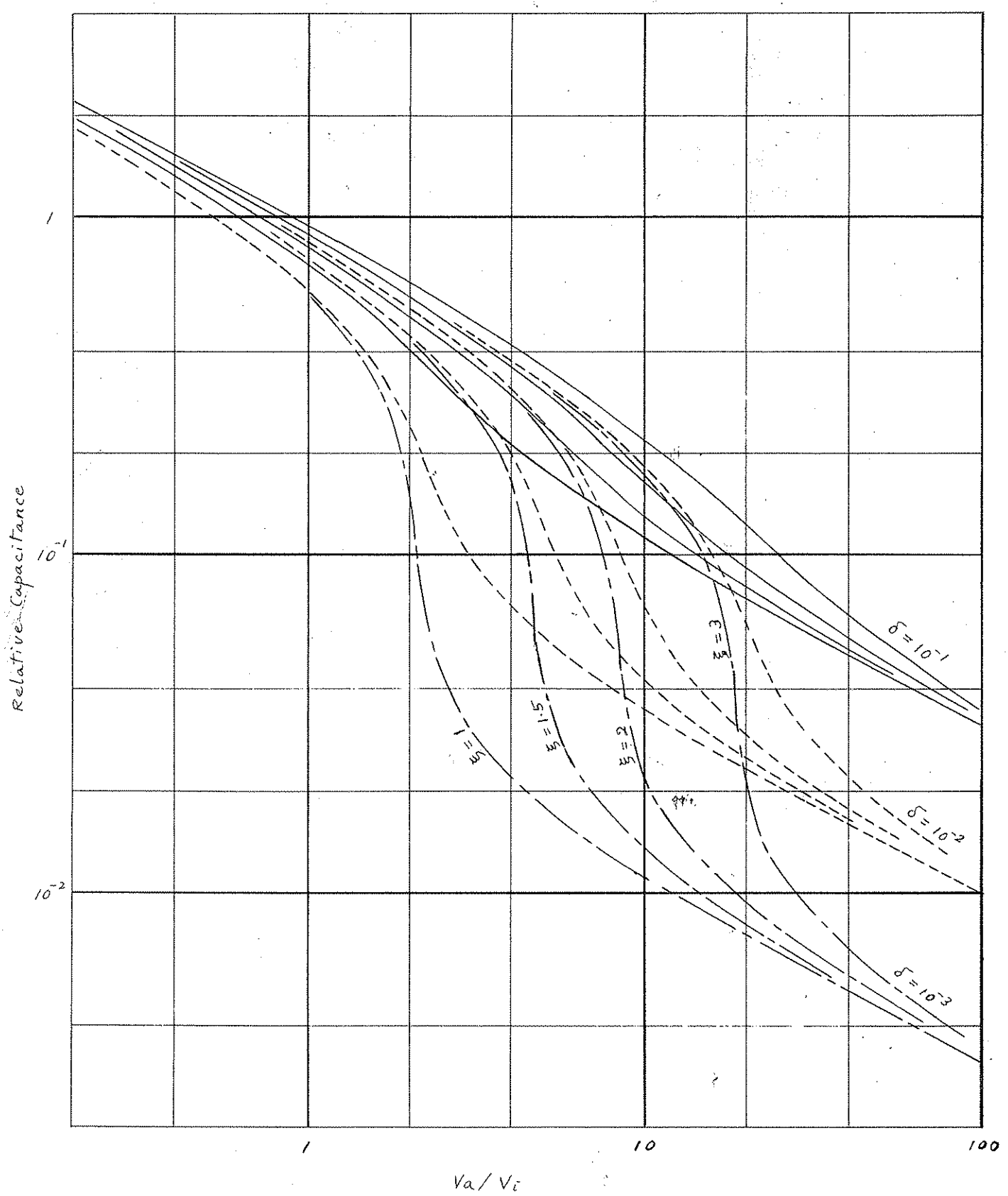

Fig. 2.3 Capacitance variation of a hyper-abrupt junction as a function of normalized junction voltage.

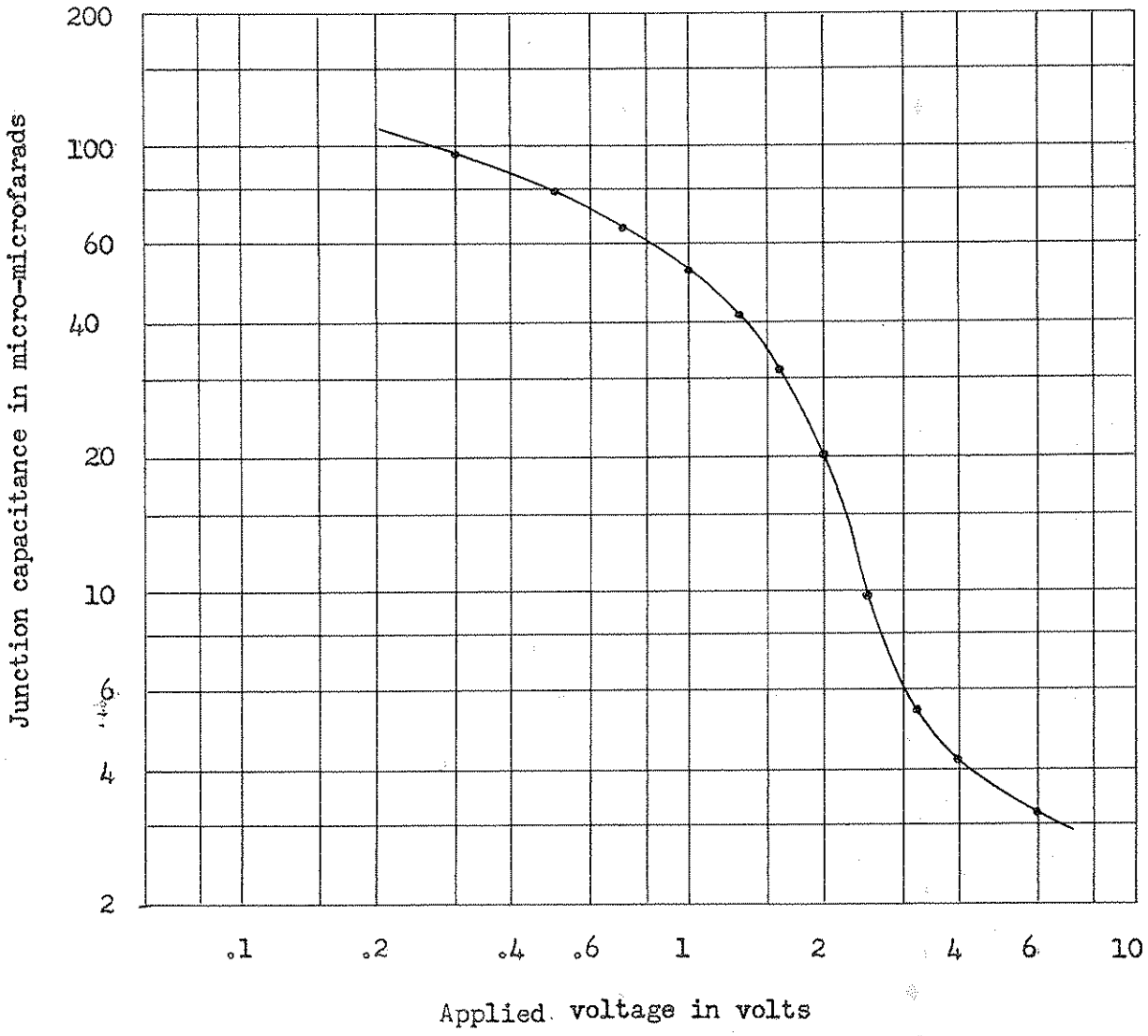

Fig. 2.4 Junction capacitance vs applied voltage relation of a hyper-abrupt junction diode.

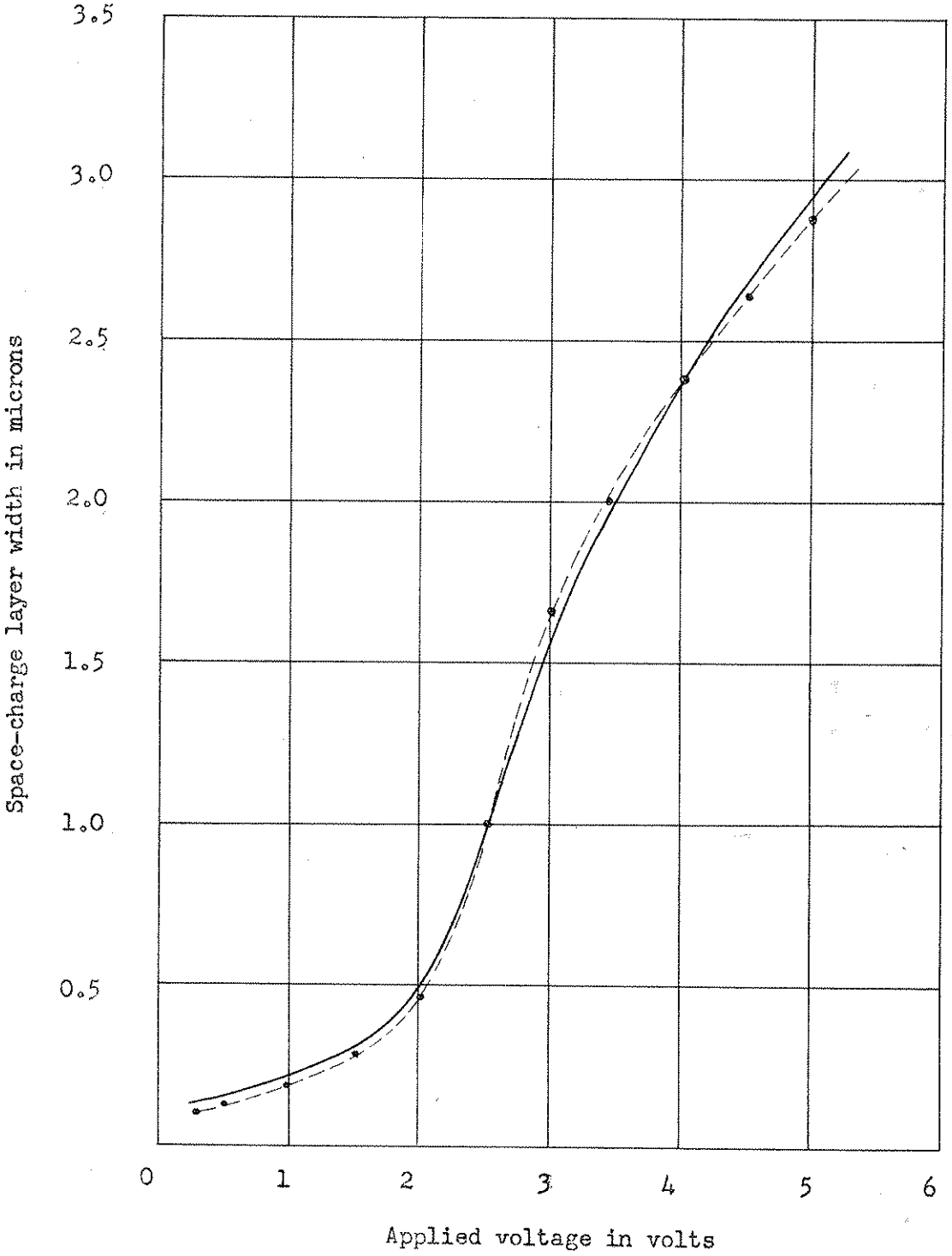

Fig. 2.5 Space-charge layer width vs applied voltage relation of a hyper-abrupt junction

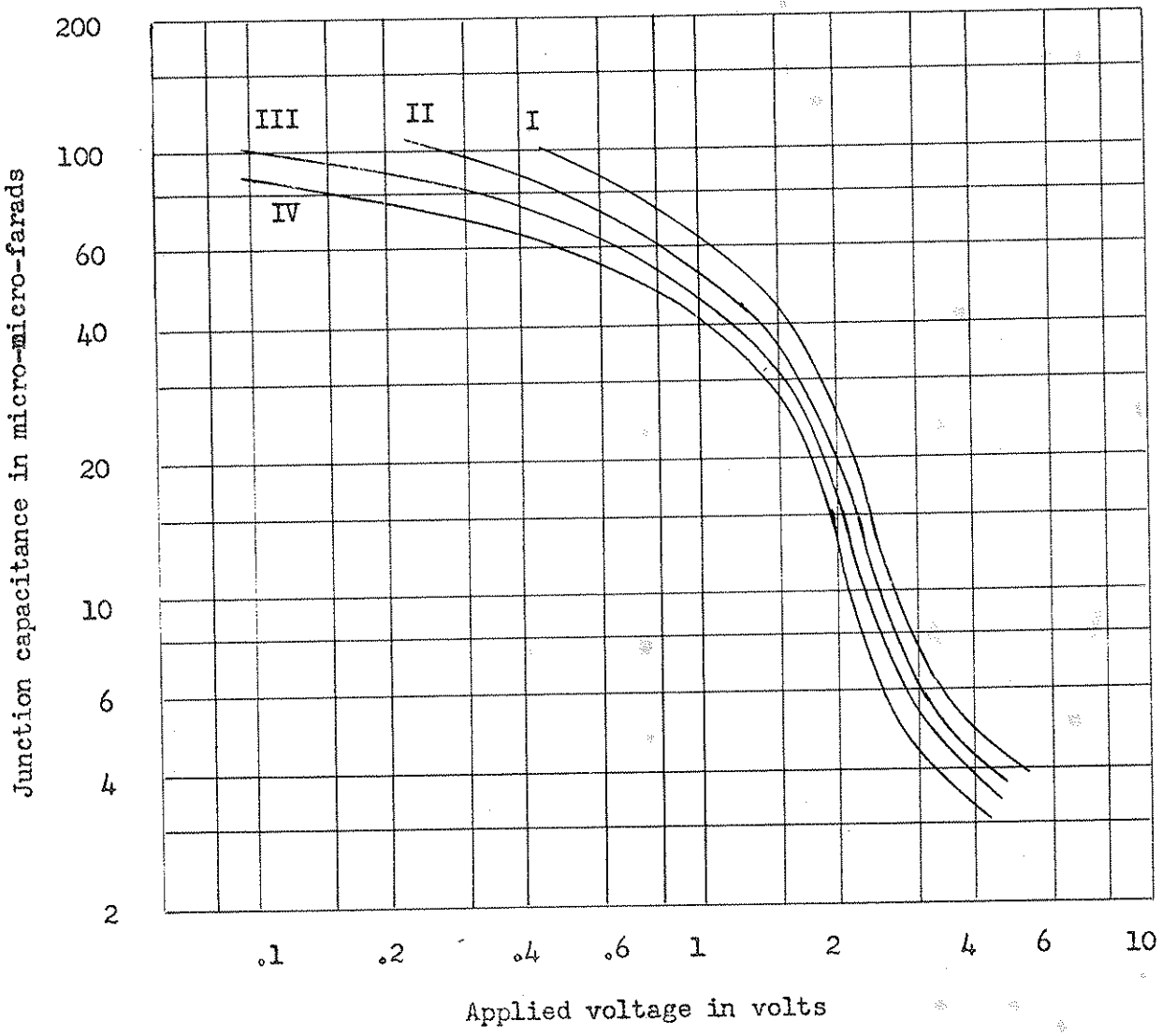

Fig. 3;1 Temperature dependence of the characteristics of junction capacitance vs applied voltage.

I: 350° K II: 300° K III: 200° K IV: 70° K

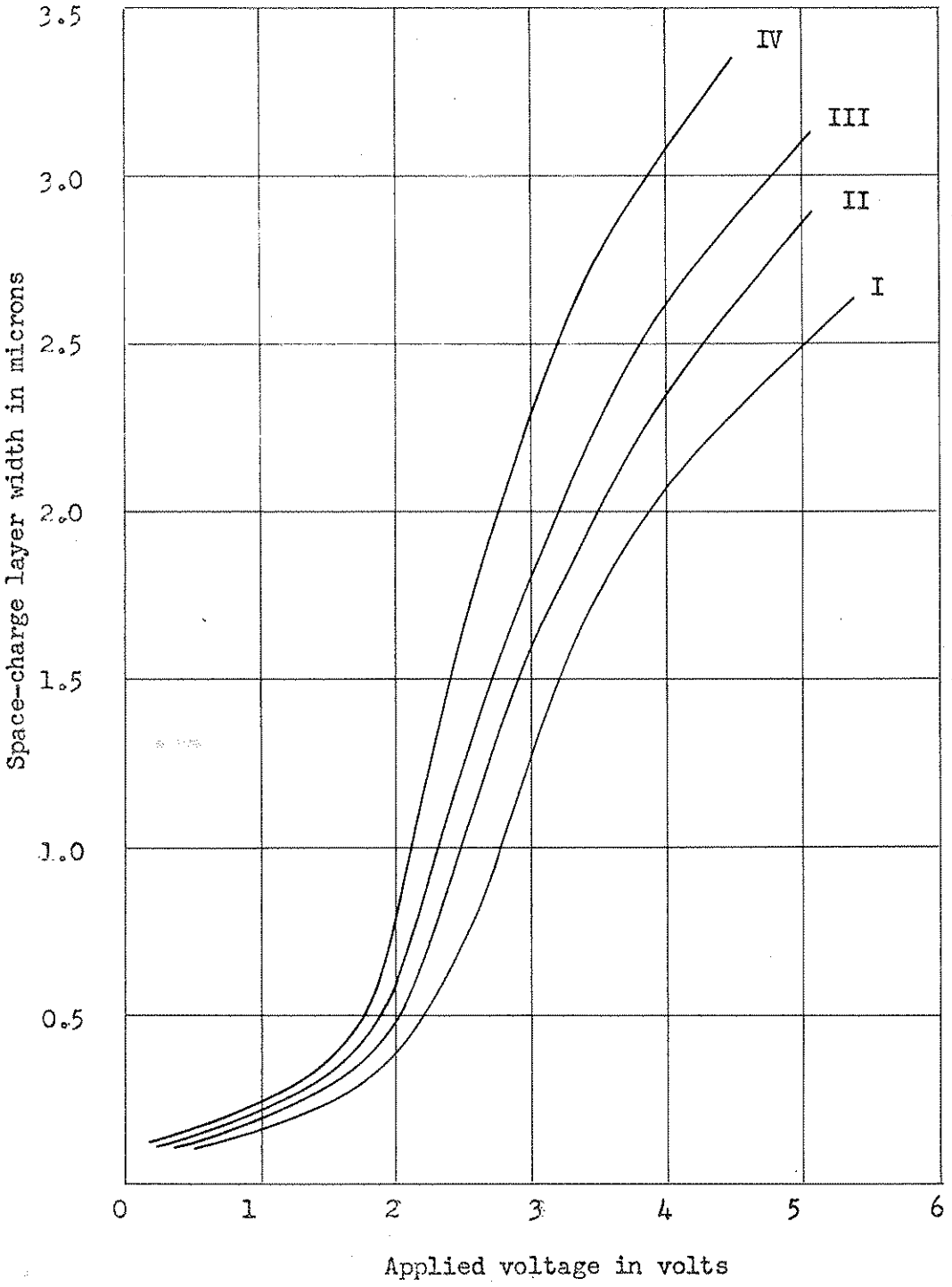

Fig. 3.2 Temperature-dependence of the characteristics of space-charge layer width vs applied voltage.

I: 350° K II: 300° K III: 200°K IV: 70° K

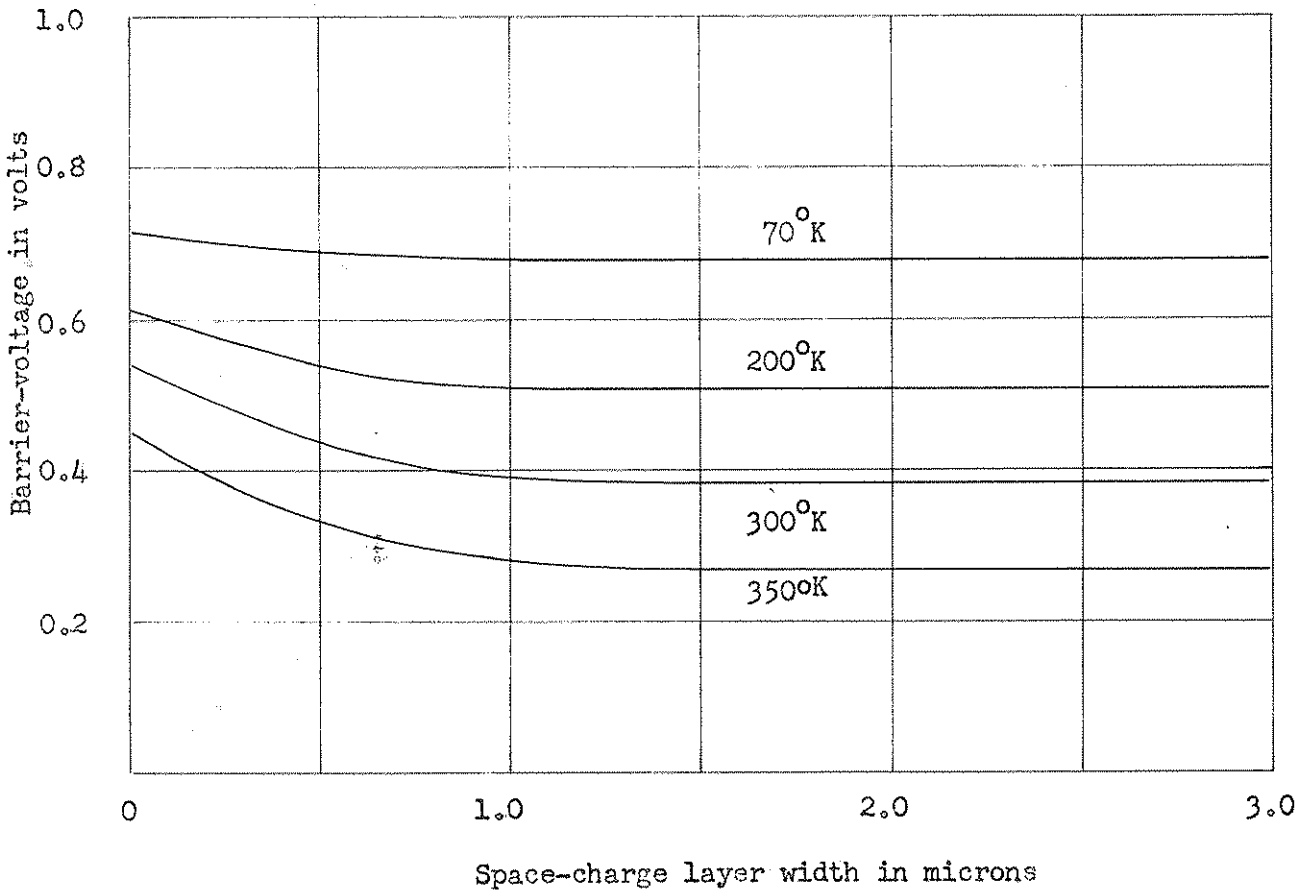

Fig. 3.3 Barrier-voltage as a function of the space-charge layer width at various temperature

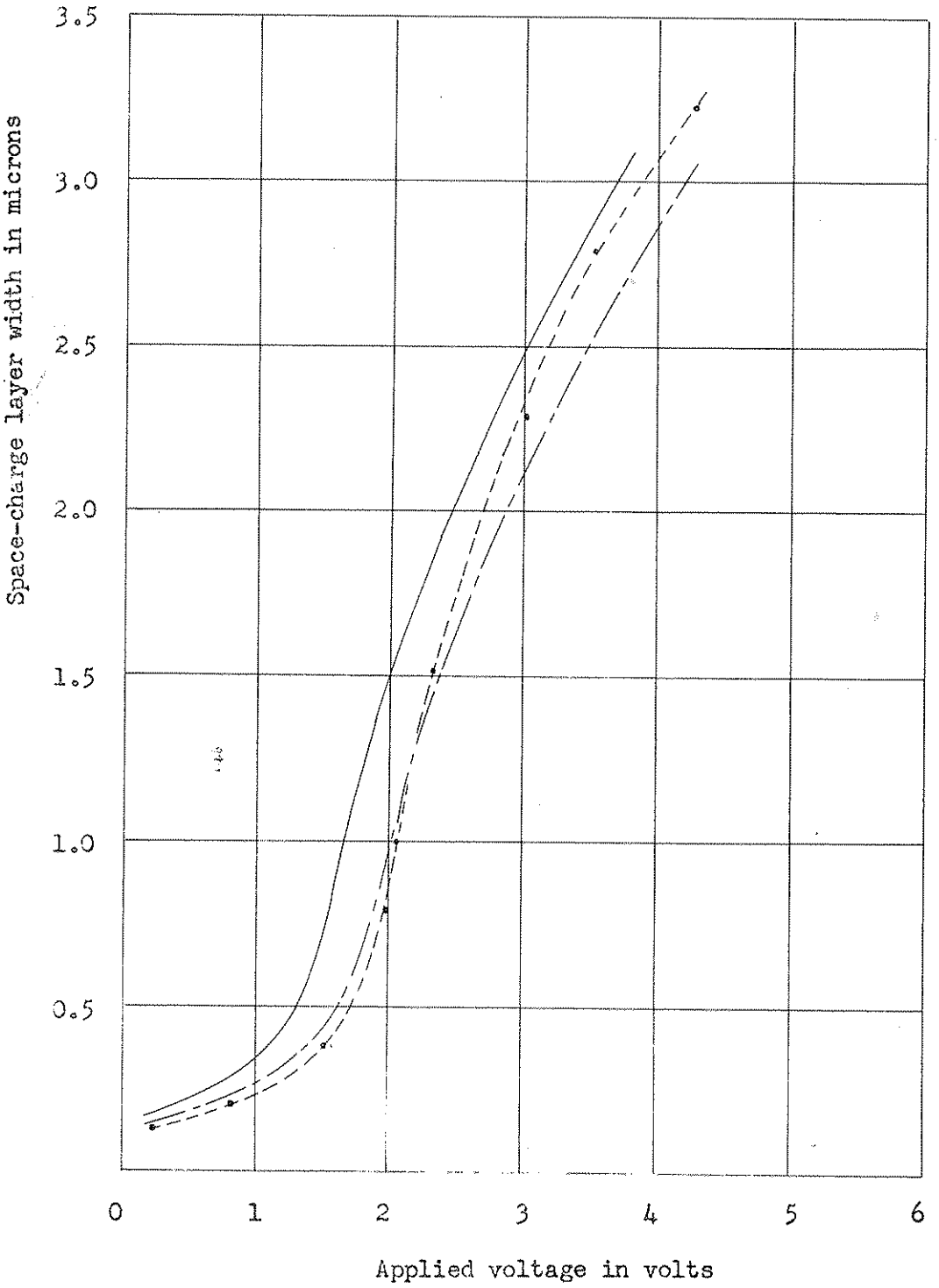

Fig. 3.4 Characteristics of the space-charge layer width vs applied voltage at 70° K.

日本無線株式会社

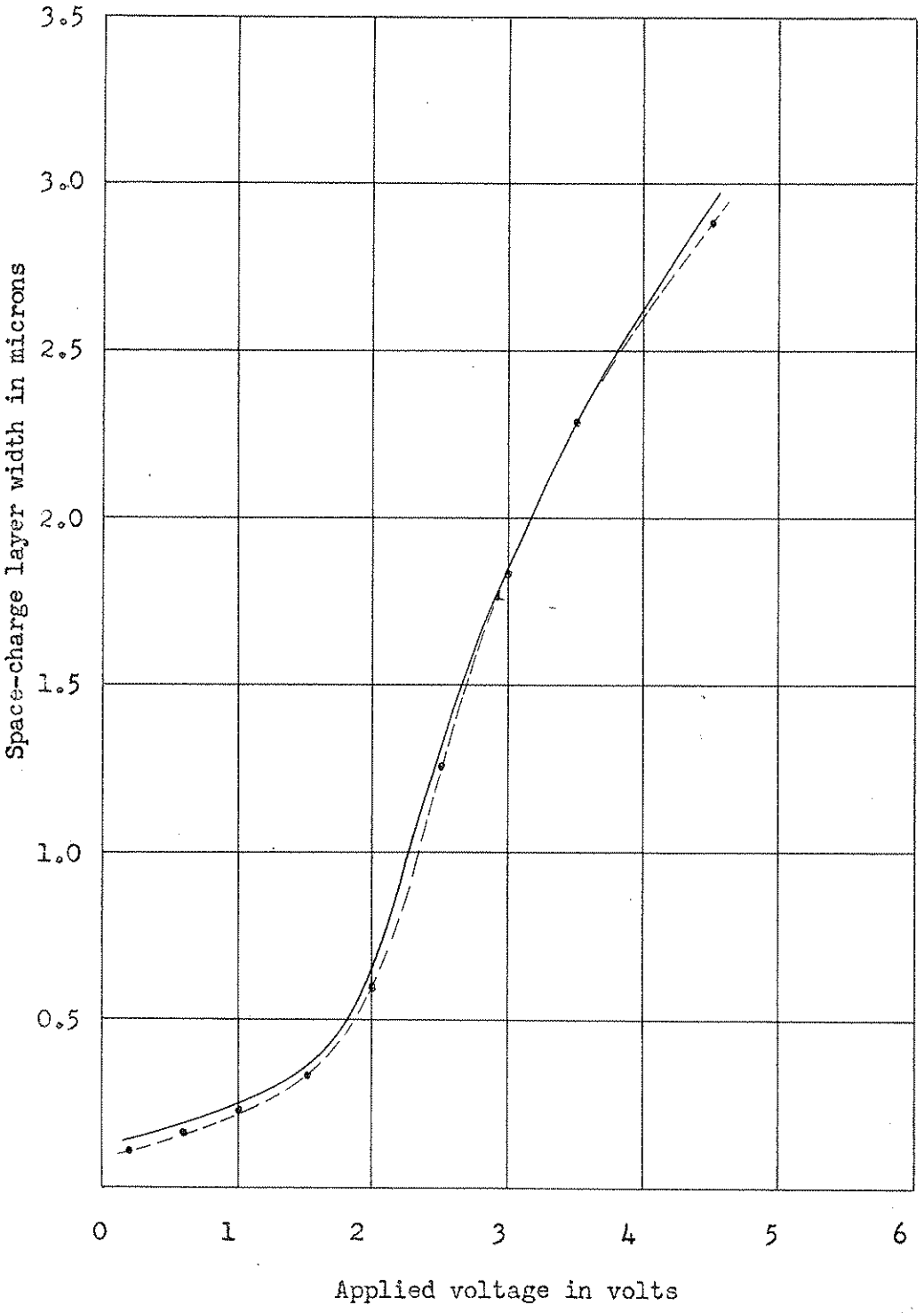

Fig. 3.5 Characteristics of the space-charge layer width vs applied voltage at 200° K

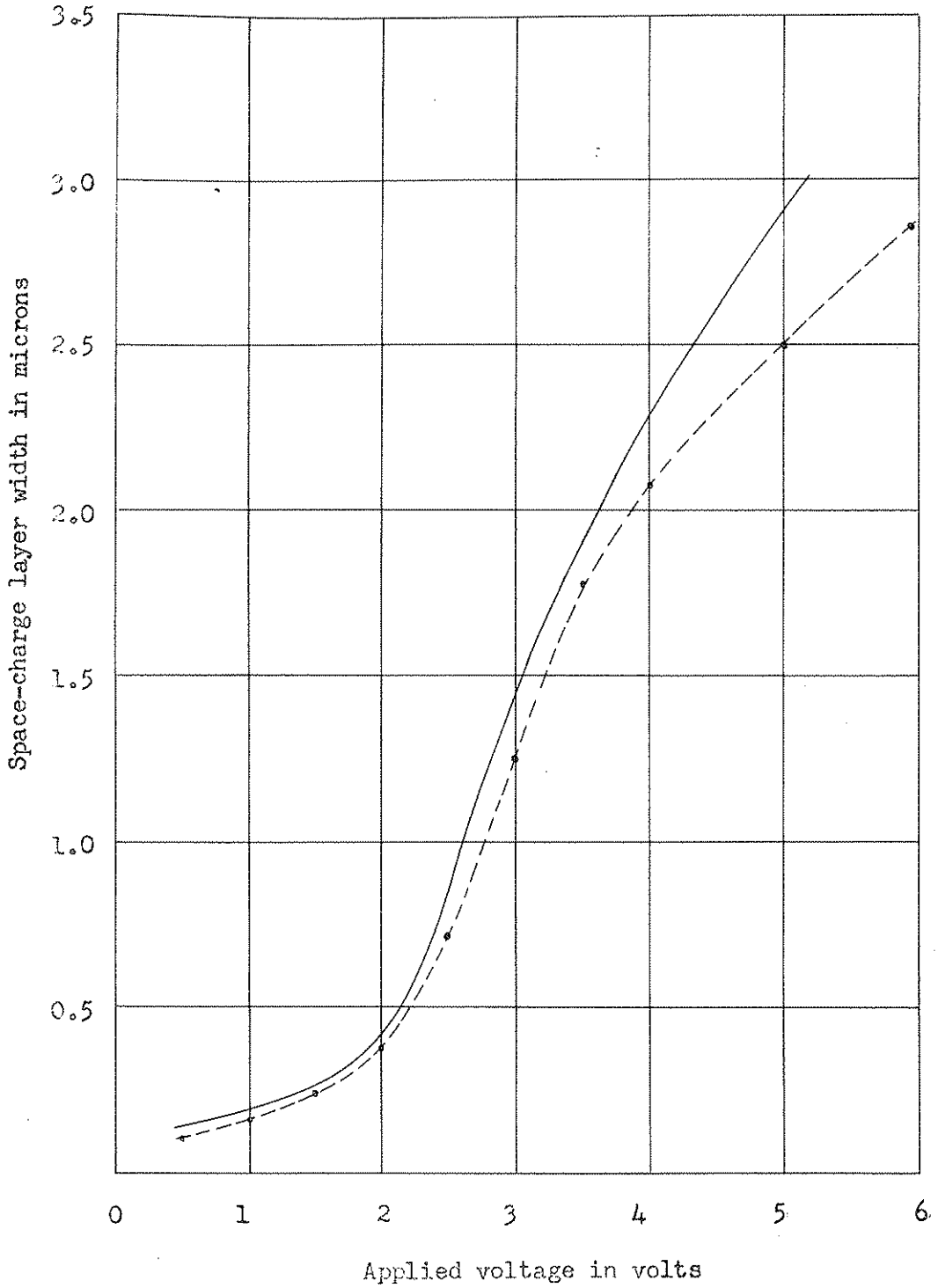

Fig. 3.6 Characteristics of the space-charge layer width vs applied voltage at 350° K.

日本無線株式会社